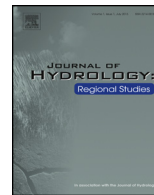




ELSEVIER

Contents lists available at [ScienceDirect](http://ScienceDirect)

# Journal of Hydrology: Regional Studies

journal homepage: [www.elsevier.com/locate/ejrh](http://www.elsevier.com/locate/ejrh)

## Effects of land cover change on evapotranspiration and streamflow of small catchments in the Upper Xingu River Basin, Central Brazil



Lívia Cristina Pinto Dias<sup>a,\*</sup>, Márcia N. Macedo<sup>b</sup>,  
Marcos Heil Costa<sup>a</sup>, Michael T. Coe<sup>b</sup>, Christopher Neill<sup>c</sup>

<sup>a</sup> The Federal University of Viçosa, Viçosa, MG 36570-900, Brazil

<sup>b</sup> The Woods Hole Research Center, 149 Woods Hole Rd, Falmouth, MA 02540, USA

<sup>c</sup> The Ecosystems Center, Marine Biological Laboratory, 7 MBL Street, Woods Hole, MA 02543, USA

### ARTICLE INFO

#### Article history:

Received 26 December 2014

Received in revised form 7 May 2015

Accepted 11 May 2015

Available online 19 June 2015

#### Keywords:

Evapotranspiration

Streamflow

Modeling

Xingu Basin

Amazon

Cerrado

### ABSTRACT

**Study region:** Upper Xingu River Basin, southeastern Amazonia.

**Study focus:** This study assessed the influence of land cover changes on evapotranspiration and streamflow in small catchments in the Upper Xingu River Basin (Mato Grosso state, Brazil). Streamflow was measured in catchments with uniform land use for September 1, 2008 to August 31, 2010. We used models to simulate evapotranspiration and streamflow for the four most common land cover types found in the Upper Xingu: tropical forest, cerrado (savanna), pasture, and soybean croplands. We used INLAND to perform single point simulations considering tropical rainforest, cerrado and pasturelands, and AgrolBIS for croplands.

**New hydrological insights for the region:** Converting natural vegetation to agriculture substantially modifies evapotranspiration and streamflow in small catchments. Measured mean streamflow in soy catchments was about three times greater than that of forest catchments, while the mean annual amplitude of flow in soy catchments was more than twice that of forest catchments. Simulated mean annual evapotranspiration was 39% lower in agricultural ecosystems (pasture and soybean cropland) than in natural ecosystems (tropical rainforest and cerrado). Observed and simulated mean annual streamflows in agricultural ecosystems were more than 100% higher than in natural ecosystems. The accuracy of the simulations was improved by using field-measured soil hydraulic properties. The inclusion of local measurements of key soil parameters is likely to improve hydrological simulations in other tropical regions.

© 2015 The Authors. Published by Elsevier B.V. This is an open access article under the CC BY-NC-ND license (<http://creativecommons.org/licenses/by-nc-nd/4.0/>).

\* Corresponding author. Tel.: +55 31 3899 1902.

E-mail addresses: [liviacrisdias@gmail.com](mailto:liviacrisdias@gmail.com) (L.C.P. Dias), [mmacedo@whrc.org](mailto:mmacedo@whrc.org) (M.N. Macedo), [mhcosta@ufv.br](mailto:mhcosta@ufv.br) (M.H. Costa), [mtcoe@whrc.org](mailto:mtcoe@whrc.org) (M.T. Coe), [cneill@mbl.edu](mailto:cneill@mbl.edu) (C. Neill).

<http://dx.doi.org/10.1016/j.ejrh.2015.05.010>

2214-5818/© 2015 The Authors. Published by Elsevier B.V. This is an open access article under the CC BY-NC-ND license (<http://creativecommons.org/licenses/by-nc-nd/4.0/>).

## 1. Introduction

The Amazon is the Earth's largest remaining tropical forest and the location of the largest absolute extent of tropical forest clearing each year. In the eastern Amazon, the Xingu River Basin has a drainage area of approximately 500,000 km<sup>2</sup>, and annual mean discharge of about 8000 m<sup>3</sup> s<sup>-1</sup>, making it the 5th largest tributary of the Amazon. The Xingu headwaters region is located in Mato Grosso state (Upper Xingu) and the river flows northward for roughly 2000 km before reaching the Amazon River in Pará state (Fig. 1a). In addition to its large extent, the Xingu Basin is economically and environmentally important. The third-largest hydroelectric dam complex in the world, the Belo Monte Dam, is currently under construction at Altamira, near the confluence of the Xingu and the Amazon River. At the same time, the Xingu Basin contains one of the world's largest mosaics of protected areas and indigenous reserves, which protect indigenous cultures and 280,000 km<sup>2</sup> of tropical forest.

High deforestation rates and rapid changes in the agricultural landscape have occurred in the Upper Xingu outside of the indigenous reserve, with about 35% of the original forest converted to pasture and croplands (especially soybeans) by 2010 (Leite et al., 2011; Macedo et al., 2012; Morton et al., 2006). These transitions from native forests and savannas to pastures or croplands drive widespread changes in vegetation that have the potential to modify the hydroclimatology of the Upper Xingu (Coe et al., 2013; Panday et al., 2015).

The classic study by Bosch and Hewlett (1982) quantified how reduction of vegetation cover increases average annual discharge. This has been confirmed for various ecosystems by Andréassian (2004), Brown et al. (2005), Bruijnzeel (1990) and Sahin and Hall (1996). Recently, Hayhoe et al. (2011) conducted a paired catchment experiment at the Tanguro Farm in the Upper Xingu (Fig. 1a) to examine how the conversion of tropical forests to soybeans influences the seasonality of streamflow and

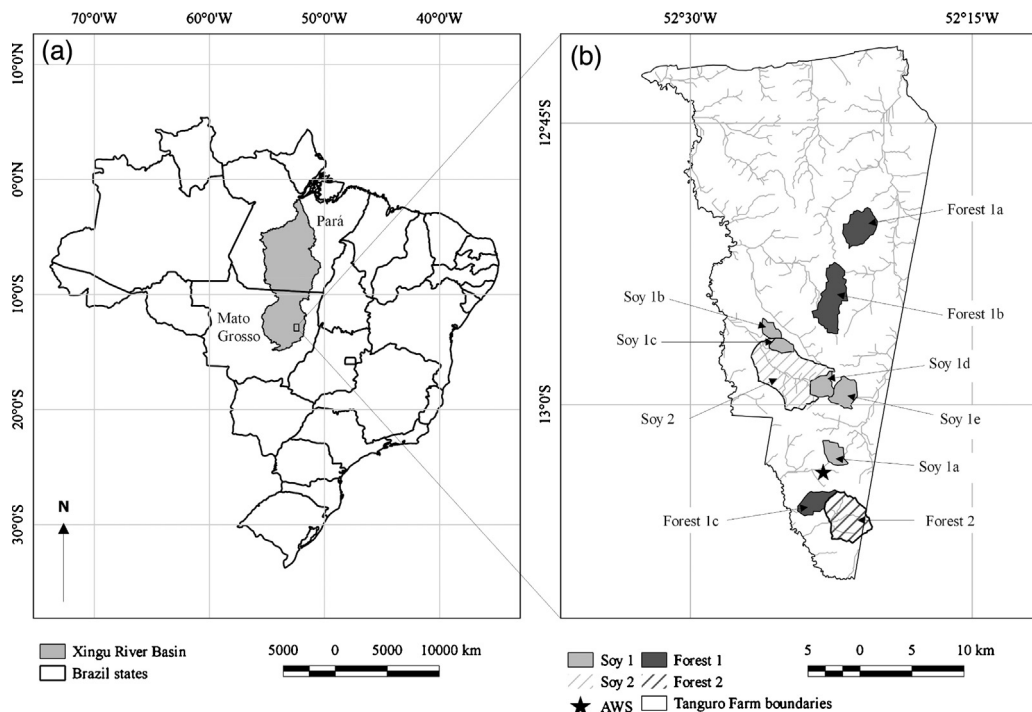


**Fig. 1.** Map of the study area. (a) Location of the Xingu River Basin and Tanguro Farm within the Amazon. (b) Inset depicting the location of the study catchments within Tanguro Farm. First-order catchments are labeled with a 1; second-order catchments are labeled with 2. The star indicates the location of the automatic weather station (AWS).

to quantify the discharge of small catchments under these two types of vegetation cover. The authors found that water yield in soybean catchments was approximately fourfold that of forest catchments and that stormflows contributed less than 13% of the annual discharge, while baseflow accounted for nearly 90% of annual streamflow in both forest and soybean catchments.

The Upper Xingu is an ideal study area for examining the effects of land cover change on hydrology because it spans the transition between evergreen tropical forest in the north and cerrado (Brazilian savanna) in the south. This transition zone provides a unique opportunity to study four types of land cover (tropical forest, cerrado, pasture and soybean) under similar climatological and edaphic conditions.

Land surface models (LSM) have been used to simulate the behavior of the hydrological system at various scales in central Brazil (Coe et al., 2011; Panday et al., 2015; Pongratz et al., 2006) and Amazonia (Coe et al., 2009; Costa and Foley, 1997). These models describe the flow of water between soil, vegetation, and atmosphere and allow researchers to investigate land surface processes (evapotranspiration, runoff and drainage), as well as the historical and potential future consequences of climate and deforestation for the regional water balance.

Since the first LSM was developed in the late 1960s, LSMs have been iteratively refined and they can be classified into generations according to the processes included, as described by Sellers et al. (1997). After the second generation, several important hydrological processes were included, such as biophysical control of evapotranspiration, precipitation interception, and soil moisture availability. Third- and fourth-generation models include improvements in carbon assimilation and dynamic vegetation, respectively, and are the most common models used in previous land use change studies in Brazil.

Costa and Foley (1997) used a modified version of the Land Surface Transfer Scheme (LSX; third-generation model; Pollard and Thompson, 1995) to analyze the water balance in the Amazon Basin. This study demonstrated that forest clearing decreases annual evapotranspiration by 12% in the Amazon Basin. Pongratz et al. (2006) used the Simple Biosphere Model (SiB2; third-generation model; Sellers et al., 1996a,b), to study the surface energy and water balance in Mato Grosso. Their results indicated that forest clearing increases the daily temperature range and that conversion of evergreen forest to C3 croplands decreases the latent heat flux by 21% during the wet season. The Integrated Biosphere Simulator (IBIS; Foley et al., 1996; Kucharik et al., 2000), a fourth-generation model, has been extensively used to study the influence of deforestation on the discharge of the Amazon River and its tributaries (Coe et al., 2011, 2009; Lima et al., 2014; Panday et al., 2015; Stickler et al., 2013). The authors found that large-scale historical deforestation has increased discharge by as much as 20% in large watersheds of the southeastern Amazon.

Independent of the model chosen, the accuracy of simulated results is fundamentally dependent on the parameters chosen. Parameters representing soil hydrological properties such as porosity, field capacity, wilting point and saturated hydraulic conductivity are particularly important because they influence soil water retention, the amount of water available for evapotranspiration (Cuenca et al., 1996; Delire et al., 1997; Marthews et al., 2014), and the resulting water cycle.

This study presents a combination of field measurements and model simulation results for the Upper Xingu focused around three main goals: (1) analysis of water yield data collected in tropical forest and soybean catchments to understand the effects of land cover change on regional water dynamics; (2) determination of the best set of soil hydrological properties for simulating the partitioning of annual precipitation into evapotranspiration and discharge in forest and soybean catchments; and (3) investigation of the differences in annual evapotranspiration and streamflow in tropical forest, cerrado, pasture and soybean catchments in the Upper Xingu.

## 2. Materials and methods

### 2.1. Site description

The study is centered on the 80,000 ha Tanguro Farm, a large soybean farm located in the Upper Xingu Basin, in Mato Grosso, Brazil (Fig. 1). This region is located in the Brazilian Central Plateau, characterized by a generally flat topography and dominated by oxisols with a mean soil texture of

55% sand, 2% silt, and 43% clay (Hayhoe et al., 2011; Scheffler et al., 2011). Tanguro was originally covered by transitional tropical forests, with an average canopy height of 20 m and relatively low species diversity compared to the wetter tropical forests occurring further north and west (Balch et al., 2008). During the 1980s, about 32,000 ha were cleared and converted to pasture grasses, consisting mostly of *Brachiaria* sp. (Scheffler et al., 2011). Between 2004 and 2008, these pasturelands were converted to mechanized soy production. This land use history is typical of much of the Upper Xingu region.

During the study period (2007–2010), soybean was planted near the onset of the rainy season (usually in November). In general, in the first year after conversion, only a single crop of soybeans was planted in the field (without crop rotation), and the soil remained exposed between growing seasons. After the first year, typically a single soybean crop was planted in November (using a no-till planting system) and harvested around March, when a cover crop (usually millet) was planted to protect the soils between growing seasons.

## 2.2. Discharge and meteorological data

Discharge was measured in twelve headwater catchments located entirely on the Tanguro Farm from September 2007 to December 2010. The study catchments included seven soybean (six first-order and one second-order) and five forested (four first-order and one second-order) streams. Because ten of these catchments were also studied by Hayhoe et al. (2011), we named them following Hayhoe et al. (2011) to facilitate comparison of results between these studies (Fig. 1b). Our study differs from Hayhoe et al. (2011) because it includes two additional catchments (one in forest and one in soybean), an 18-month longer time series, and updated rating curves.

Discharge was estimated based on hourly water level data, following the methods described in Hayhoe et al. (2011). Briefly, each basin was gauged with a staff gauge and Onset HOBO U20 Water Level data logger, which monitored hourly barometric pressure. Pressure data was converted to water level (depth) using reference air pressure data (logged with an identical unit in a nearby field laboratory) and calibrated using the permanent staff gauges at each site. Finally, the entire water level time series, including the catchments and time periods reported by Hayhoe et al. (2011), was converted to discharge using updated rating curves. The depth-to-discharge relationships were developed for each catchment based on periodic discharge measurements using a Marsh McBirney Flo-Mate 2000 electromagnetic flow meter. Catchment boundaries were delineated based on vegetation-corrected Shuttle Radar Topography Mission (SRTM) data, using standard hydrology tools in ESRI ArcGIS 10.2.

Hourly temperature, humidity, wind speed, rainfall, and incoming solar radiation data were measured by an automatic weather station (AWS, Fig. 1b) located inside the Tanguro Farm (Latitude: 13°37'16" S; Longitude: 52°22'55.68" W; altitude: 358 m), between January 2007 and December 2011. Where necessary (typically before September 2008) we used the PERSIANN (*Precipitation Estimation from Remotely Sensed Information using Artificial Neural Networks*; Hsu et al., 1997; Sorooshian and Hsu, 2000) 0.25° global precipitation dataset to fill gaps in the rainfall time series. Missing values for the other variables were filled following the same behavior of the previous adjacent data points.

Incident longwave radiation ( $L_{in}$ ) is an input variable required to run the INLAND and Agro-IBIS models (described in Section 2.3). Although it was not measured directly by the Tanguro AWS,  $L_{in}$  can be estimated from other measured meteorological variables using previously published equations (Brutsaert, 1975; Idso and Jackson, 1969; Idso, 1981; Prata, 1996; Satterlund, 1979), which are only valid for clear sky conditions. Here, we estimated  $L_{in}$  for all days of the simulation period according to the empirical equation proposed by Idso (1981), which uses the Stefan–Boltzmann constant ( $\sigma$ ), air temperature ( $T$ ) in Kelvin and water vapor pressure ( $e$ ) in kPa:

$$L_{in} = [0.7 + 5.95 \times 10^{-5}(e \exp(1500/T))] \sigma T^4$$

We assume that the errors associated with  $L_{in}$  estimation influenced all simulations equally, enabling analysis of the relative differences in the behavior of the simulated water balance. We

chose the [Idso \(1981\)](#) equation because it showed the best agreement with measurements of incident longwave radiation in pasture and forest sites in southwestern Amazonia ([Aguiar et al., 2011](#)).

### 2.3. Numerical experiment

The Integrated Model of Land Surface Processes (INLAND; Costa et al., manuscript in preparation) is a fifth-generation model that has been developed by Brazilian researchers as part of the Brazilian Earth System Model project. This model is an evolution of the IBIS. One of the main goals of the INLAND project is to better represent biomes and important processes in Brazil (such as agriculture). To include agriculture, the Dynamic Model of Agroecosystems (AgroIBIS) is being incorporated into INLAND. AgroIBIS is a modified version of IBIS capable of simulating phenological and physiological characteristics of crops ([Kucharik and Twine, 2007](#); [Kucharik, 2003](#)). Because the integration of these two models was underway when we performed the simulations in this study, we elected to use INLAND version 1.0 and AgroIBIS separately. Because both models are modifications of IBIS, they share most water balance equations and their results are directly comparable in the context applied here.

These models simulate the exchanges of energy, water, carbon and momentum in the soil–vegetation–atmosphere system. They represent two layers of vegetation with 12 plant functional types, as well as six soil layers of variable thickness, representing a total of 8 m in depth. Water infiltration in soil is modeled using Darcy's equation and soil moisture is based on the flow of Richards's equation. Plant transpiration is governed by stomatal conductance coupled to photosynthesis ([Ball et al., 1987](#)). Total evapotranspiration is the sum of bare soil evaporation, plant transpiration and evaporation from precipitation intercepted by the canopy ([Pollard and Thompson, 1995](#)). Water uptake by plants is a function of atmospheric demand, soil physical properties, root distribution and water in the soil profile ([Kucharik et al., 2000](#)). Finally, surface and subsurface runoff are explicitly simulated as a function of the water not evapotranspired to the atmosphere (i.e. the difference between rainfall and total evapotranspiration), soil characteristics, vegetation and climate.

We performed single point simulations for tropical forest, cerrado, and pasture land uses in the INLAND model and soybean cropland in the AgroIBIS model. Although we ran the models for the period from January 1, 2007 to December 31, 2011, we analyzed simulation results only for two hydrological years (September 1, 2008 to August, 31 2010). Hourly meteorological data from the AWS at Tanguro Farm served as model input data and we considered it representative for all catchments in the study. We used fixed vegetation for the natural ecosystems (cerrado and forest) and pastureland simulations. We specified November 1st as the planting date for single-cropped soybeans and assumed that soils remained exposed in the periods between plantings. We used fixed concentrations of CO<sub>2</sub> at 390 ppm in all simulations.

### 2.4. Soil hydrological properties

Soil properties in INLAND and AgroIBIS are based on soil texture, and the soil at Tanguro Farm is classified as sandy clay according to the USDA soil texture triangle. Here, we considered three potential data sources to describe the hydrological properties of sandy clay soils: the mean values described by [Campbell and Norman \(1998\)](#), the pedotransfer functions proposed by [Cosby et al. \(1984\)](#) and observed data for Tanguro Farm described by [Scheffler et al. \(2011\)](#).

INLAND and AgroIBIS currently use values for porosity ( $\Theta_s$ ), field capacity ( $\Theta_{fc}$ ), wilting point ( $\Theta_{wp}$ ), Campbell's "b" exponent ( $b$ ), air entry potential ( $\Psi_{ad}$ ) and saturated hydraulic conductivity ( $K_s$ ), as recommended by [Campbell and Norman \(1998\)](#). Recently, however, hydrologic properties of soils estimated using pedotransfer functions based on soil texture, proposed by [Cosby et al. \(1984\)](#), have been used by the Large-Scale Biosphere–Atmosphere Experiment in Amazonia Data Model Inter-comparison Project (LBA-DMIP; [De Gonçalves et al., 2013](#)). In addition, [Scheffler et al. \(2011\)](#) measured in situ values of  $K_s$  under forest, pasture and soybean covers on Tanguro Farm.

For each land cover (forest, cerrado, pasture, and soybean), we assessed four sets of soil hydraulic parameters to identify the combination that provides the smallest difference between simulated data

**Table 1**

Soil sand-clay parameters used for simulations A (all parameters from Cosby et al., 1984), B ( $K_S$  from Scheffler et al., 2011; other parameters from Cosby et al., 1984), C (all parameters from Campbell and Norman, 1998) and D ( $K_S$  from Scheffler et al., 2011; other parameters from Campbell and Norman, 1998).  $\Theta_s$ , porosity ( $\text{m}^3 \text{m}^{-3}$ );  $\Theta_{fc}$ , field capacity ( $\text{m}^3 \text{m}^{-3}$ );  $\Theta_{wp}$ , wilting point ( $\text{m}^3 \text{m}^{-3}$ );  $b$ , Campbell's "b" exponent;  $\Psi_{ad}$ , air entry potential (mH<sub>2</sub>O); and  $K_S$ , saturated hydraulic conductivity ( $\text{m s}^{-1}$ ).

Simulation	Land Cover	$\Theta_s$	$\Theta_{fc}$	$\Theta_{wp}$	$b$	$\Psi_{ad}$	$K_S$
A	All	0.411	0.284	0.194	9.7	0.18	$4.638 \times 10^{-6}$
B	Forest/Cerrado	0.411	0.242	0.194	9.7	0.18	$1.565 \times 10^{-4}$
	Pasture	0.411	0.262	0.194	9.7	0.18	$2.781 \times 10^{-5}$
	Soy	0.411	0.260	0.194	9.7	0.18	$3.189 \times 10^{-5}$
C	All	0.430	0.339	0.239	6.0	0.29	$3.333 \times 10^{-7}$
D	Forest/Cerrado	0.430	0.339	0.239	6.0	0.29	$1.565 \times 10^{-4}$
	Pasture	0.430	0.339	0.239	6.0	0.29	$2.781 \times 10^{-5}$
	Soy	0.430	0.339	0.239	6.0	0.29	$3.189 \times 10^{-5}$

and mean observed values for forest and soybeans (Table 1). The four resulting simulation scenarios were:

- A. All soil hydraulic parameters estimated using Cosby et al. (1984) equations;
- B.  $K_S$  measured at the Tanguro Farm (Scheffler et al., 2011) and other parameters estimated using Cosby et al. (1984) equations;
- C. All soil hydraulic parameters recommended by Campbell and Norman (1998);
- D.  $K_S$  measured at the Tanguro Farm (Scheffler et al., 2011) and other parameters recommended by Campbell and Norman (1998).

We assume identical  $K_S$  for forest and cerrado (Table 1), since both are natural ecosystems.

### 3. Results

#### 3.1. Observed data

Observed mean annual streamflow from September 2008 to August 2010 was approximately three times higher in soybean catchments than in forest catchments (Table 2). Average total observed runoff was  $534.8 \pm 214.7 \text{ mm yr}^{-1}$  for soybean catchments (95% confidence interval (CI), 320.1–749.5  $\text{mm yr}^{-1}$ ) and  $194.6 \pm 144.1 \text{ mm yr}^{-1}$  for forest catchments (CI, 50.5–338.7  $\text{mm yr}^{-1}$ ).

**Table 2**

Average observed total runoff ( $R_{obs}$ ), runoff coefficient (C) and area of six soy catchments and four forest catchments in Tanguro Farm. Soy 1 and Forest 1 are first order catchments; Soy 2 and Forest 2 are second order catchments. Catchments that overlap with Hayhoe et al. (2011) are indicated with an asterisk.

Land cover	$R_{obs}$ ( $\text{mm yr}^{-1}$ )	C	Drainage area ( $\text{km}^2$ )
Soy 1a*	470.9	0.36	3.7
Soy 1b*	994.6	0.76	2.3
Soy 1c*	457.3	0.35	2.5
Soy 1d*	441.8	0.34	4.1
Soy 1e	125.1	0.10	5.6
Soy 2*	719.0	0.55	27.1
Mean	534.8	0.41	–
Forest 1a*	238.1	0.18	8.4
Forest 1b*	45.8	0.04	12.7
Forest 1c*	78.5	0.06	5.2
Forest 2	415.9	0.32	15.2
Mean	194.6	0.15	–

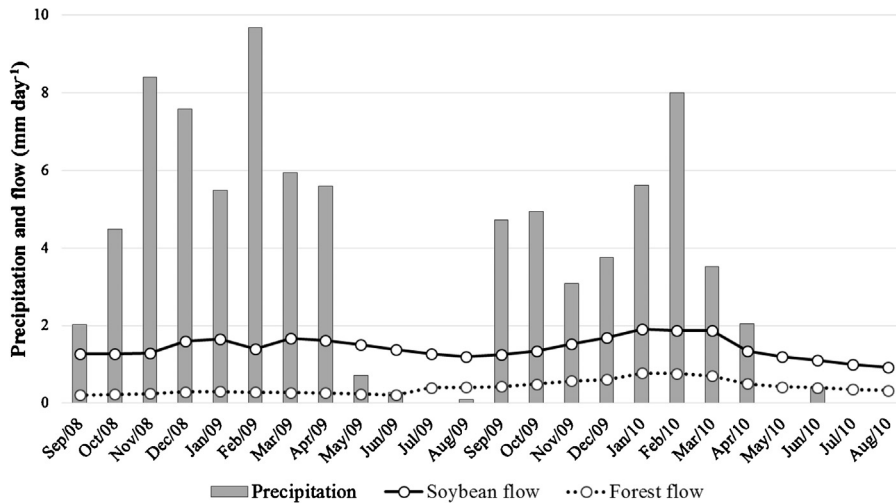


Fig. 2. Precipitation and mean daily total runoff for forest and soybean catchments in the Upper Xingu (time period September 2008 and August 2010).

During this period, the average rainfall was  $1301 \text{ mm yr}^{-1}$ . The ratio between the average annual total runoff and average annual rainfall (runoff coefficient,  $C$ ) was 0.41 (standard deviation,  $SD = 0.20$ ) in soybean catchments and 0.15 ( $SD = 0.11$ ) in forest catchments (Table 2).

The dry and wet seasons were well separated, with the wet season occurring between September and April and the dry season between May and August (Fig. 2). Mean precipitation during the wet and dry months was  $5.9$  and  $0.1 \text{ mm day}^{-1}$ , respectively. The average maximum streamflows in the two hydrological years was  $1.8 \text{ mm day}^{-1}$  for soybean catchments and  $0.6 \text{ mm day}^{-1}$  for forest catchments. The mean annual amplitude of the flow (the mean difference between maximum and minimum streamflows) in soybean catchments ( $0.7 \text{ mm day}^{-1}$ ) was more than twice that of forest catchments ( $0.3 \text{ mm day}^{-1}$ ).

### 3.2. Simulated results

The difference between mean total precipitation (Fig. 3 dashed line) and the sum of the three simulated components of the water balance (evapotranspiration, surface runoff and subsurface runoff) was the mean net change in groundwater storage (Fig. 3). The mean annual groundwater storage term was negative for all simulated sets of parameters and land covers, except for soybeans in simulation C. Negative groundwater storage meant that there was a net removal of water stored in the soil during the analyzed period. The simulated annual discharge (total runoff) was the sum of simulated annual surface and subsurface runoffs.

Simulation B predicted the smallest difference between simulated data and the mean observed values for both forest and soybeans (Fig. 4). Moreover, for soybean catchments, simulations A, B, and C predict simulated total runoff within the range of observed discharge, but only simulation B predicts total runoff within the observed range for forest catchments. Therefore, simulation B was used to analyze the effect of land cover change on evapotranspiration and streamflow in the Upper Xingu Basin. Unless otherwise noted, henceforth all simulated results refer to simulation B.

Simulated evapotranspiration was 39% lower (Table 3) in agricultural ecosystems (pasture and soybean) compared with natural ecosystems (tropical forest and cerrado). Simulated mean annual total runoff for soybean cover was twice that of forest cover. Considering the four types of land use, the mean annual simulated streamflow in agricultural ecosystems (pasture and soybeans) was 114% higher than in natural ecosystems (forest and cerrado).

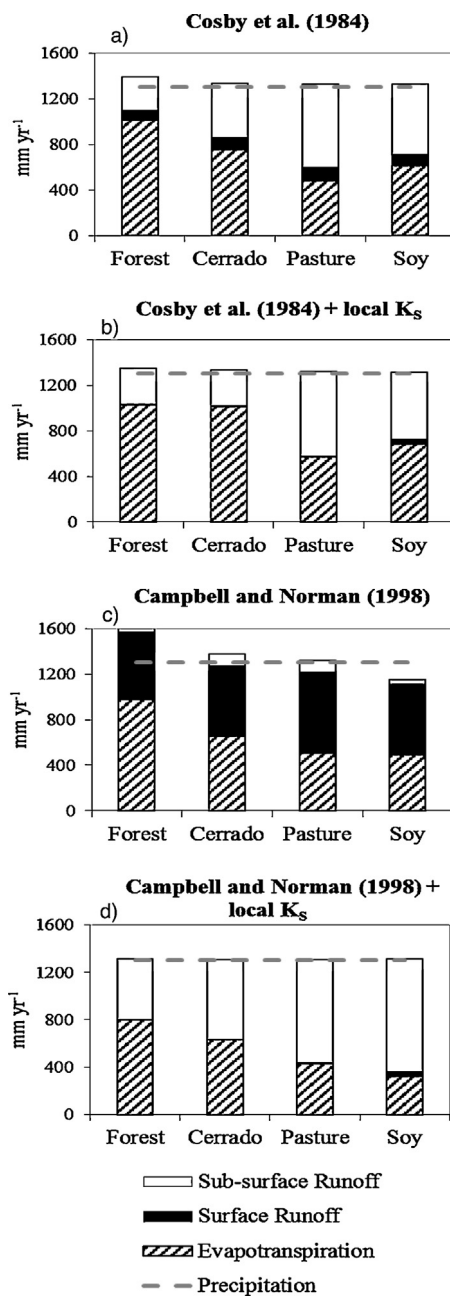


**Fig. 3.** Simulated water balance with different soil hydraulic parameters. The difference between mean total precipitation ( $1301 \text{ mm yr}^{-1}$ , dashed line) and the sum of the three simulated components of the water balance is the mean net change in groundwater storage. Simulations with (A) all parameters estimated using Cosby et al. (1984); (B)  $K_s$  measured at Tanguro Farm by Scheffler et al. (2011) and the other parameters estimated using Cosby et al. (1984); (C) the values of Campbell and Norman (1998) were used for all parameters; and (D)  $K_s$  measured at Tanguro Farm by Scheffler et al. (2011) and Campbell and Norman (1998) values in the other parameters.



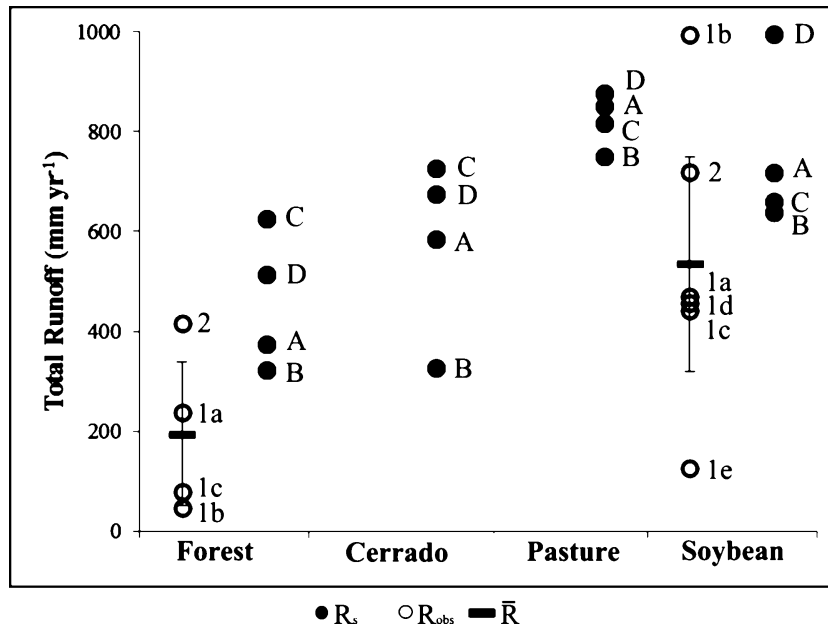


**Fig. 4.** Mean annual discharges observed ( $R_{obs}$ ), mean of  $R_{obs}$  ( $\bar{R}$ ) for each land cover, and mean annual discharge simulated ( $R_s$ ) for each land cover and four sets of soil hydraulic parameters for sandy clay soil. Small letters define catchments with forest or soy (Fig. 1 and Table 1) and capital letters define the different set of soil hydraulic parameters. Error bars indicate the confidence interval at 95%.

**Table 3**

Water balance predicted by simulation B ( $K_s$  from Scheffler et al., 2011; other parameters from Cosby et al., 1984) for the period from September 2008 and August 2010 ( $\text{mm yr}^{-1}$ ). The mean precipitation in this period was  $1301 \text{ mm yr}^{-1}$ .

	Evapotranspiration	Surface runoff	Subsurface runoff	Total runoff	Net change in groundwater storage
Forest	1024.7	0.2	322.3	322.5	-46.7
Cerrado	1009.5	0.2	324.9	325.1	-34.1
Mean	1017.1	0.2	323.6	323.8	-40.4
Pasture	567.3	5.5	744.2	749.7	-16.6
Soy	678.5	43.3	594.3	637.6	-15.6
Mean	622.9	24.4	669.3	693.7	-16.1

Simulated surface runoff was greater in agricultural ecosystems than in natural ecosystems (Table 3). Subsurface runoff represented 99% of the total runoff in the simulation with forest cover, compared to 93% for soybean cover. Considering all simulated land uses, subsurface runoff represented 96% of total runoff in agricultural ecosystems and approximately 100% of total runoff in natural ecosystems. Although the simulated surface runoff was slightly greater in agricultural ecosystems than in natural ecosystems, most of the increase in mean annual discharge was due to an increase in groundwater flow. The runoff coefficients for forest, cerrado, pasture and soybeans catchments were 0.25, 0.25, 0.58 and 0.49, respectively.

#### 4. Discussion

By combining field measurements in paired catchments with numerical modeling, our results provide insights into how the conversion of tropical forest or cerrado to pasture or soybean alters the

partitioning of rainfall into evapotranspiration and streamflow. We found that replacement of native vegetation with other land covers substantially increased water yield, which supports the results of several previous studies (Andréassian, 2004; Bosch and Hewlett, 1982; Brown et al., 2005; Bruijnzeel, 1990; Hayhoe et al., 2011; Sahin and Hall, 1996; Tomasella et al., 2009). Mean annual observed streamflow was three times larger in soybean catchments than in forest catchments, primarily because of decreased evapotranspiration. The lower leaf area index (LAI), shallower root depth, higher albedo, lower surface roughness and lower transfer of energy and momentum all contribute to reducing evapotranspiration in soybean areas (Bonan et al., 1992; Costa and Foley, 2000; Costa et al., 2007; Pongratz et al., 2006; Sampaio et al., 2007).

The variability in observed discharge among Upper Xingu catchments of comparable land use cannot be fully explained by stream slope or catchment area (Hayhoe et al., 2011). Based on our simulated results, which examined the impact of different  $K_S$  on forest discharge, and field measurements of discharge in the Forest 1a and 1b catchments, we conclude that soil properties alone cannot explain the discharge variability between sites. Total simulated runoff decreased exponentially with increasing  $K_S$  in forest sites, converging to roughly  $300 \text{ mm yr}^{-1}$ . A simulation using  $K_S$  100-times smaller than that measured in situ resulted in a simulated discharge only twice as high that under simulation B conditions. Although these results suggest that flow should vary significantly with changes in  $K_S$ , Scheffler et al. (2011) reported no significant difference in  $K_S$  at the Forest 1a and 1b catchments. Despite similar soil hydraulic characteristics, Forest 1a discharge was fivefold that of Forest 1b (Table 2).

Having eliminated  $K_S$ , stream slope, and catchment area as major contributing factors, we conclude that other factors account for the large difference in discharge. Possible causes of this variability include measurement errors, underflow beneath the monitored streams and flow between the basins (Hayhoe et al., 2011). This phenomenon is possible in flat landscapes with deep well-drained soils (Bruijnzeel, 1990) like those found in the Upper Xingu, but we were unable to refute or confirm it in this study.

The partitioning of total runoff into surface and sub-surface components was considerably altered with measured  $K_S$ . The Campbell and Norman (1998) and Cosby et al. (1984) pedotransfer equations underestimate  $K_S$  compared to the field measurements reported by Scheffler et al. (2011). This is likely because these equations were developed to predict temperate soil properties and poorly represent the behavior of tropical soils. Unlike temperate soils, tropical oxisols are highly leached, are predominantly 1:1 clay minerals and have high concentrations of aluminum and iron oxides (Barros and van Lier, 2014). Aluminum and iron oxides are the primary stabilizing agents for soil aggregates and well-aggregated soils are well-drained. Because the two indirect sources of soil properties data used in this study did not represent the well-drained sandy clay soils typical of our study area, the simulations relying exclusively on using only Campbell and Norman (1998) or Cosby et al. (1984) resulted in a greater difference between simulated data and observed runoff, compared with simulations that partially included field measurements of soil characteristics. Simulation B included the measured  $K_S$  and better represented the water balance components for the Upper Xingu.

In simulation B, evapotranspiration was  $1025 \text{ mm yr}^{-1}$  for forest and  $1010 \text{ mm yr}^{-1}$  cerrado. The forests at Tanguro Ranch occur at the transition between the Cerrado and Amazon biomes and are characterized by shorter stature and lower LAI than the dense forests found in northern Amazonia (Balch et al., 2008). Studies of similar transitional forests in Sinop (Costa et al., 2010; Vourlitis et al., 2008, 2002) estimated evapotranspiration rates ranging from  $822$  to  $1300 \text{ mm yr}^{-1}$ . For dense cerrado physiognomies (*cerradão*) and cerrado *sensu stricto*, tree-dominant savannahs expected along the Amazon-Cerrado ecotone, previous studies suggest evapotranspiration ranging from approximately  $800$  to  $1442 \text{ mm yr}^{-1}$  (Giambelluca et al., 2009; Oliveira et al., 2005). Our simulated evapotranspiration for both forest and cerrado was well within the range of those previously reported in the literature.

Our simulation results indicate that evapotranspiration was similar in forest and cerrado catchments. This is consistent with previous findings, which suggest that transitional forests and cerrados can have similar evapotranspiration if surface soil water availability is sufficient (Rodrigues et al., 2014). Tropical forests and cerrados thus exhibit similar evapotranspiration in transitional areas, given that both were constrained by the same climate and water availability during our simulations.

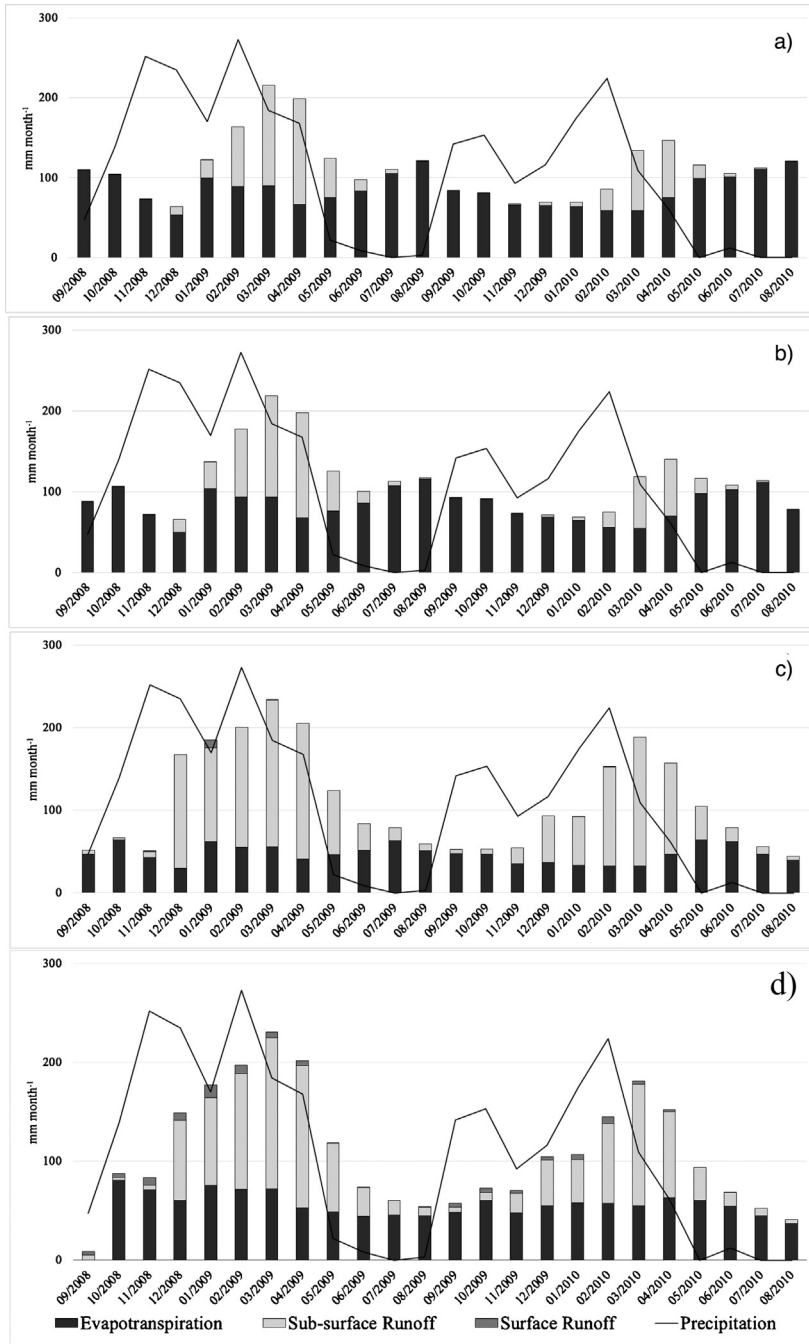


**Fig. 5.** Observed precipitation and simulated evapotranspiration, surface runoff and sub-surface runoff seasonality for (a) tropical forest, (b) cerrado, (c) pasture, and (d) soybeans in mm month<sup>-1</sup>. The difference between monthly precipitation (solid line) and the sum of the three simulated components of the water balance (vertical bars) is equal to the net change in soil water storage (positive numbers represent soil water recharge; negative numbers represent soil water depletion).

Our simulated pasture evapotranspiration ( $567 \text{ mm yr}^{-1}$ ) was lower than values previously reported in the literature for this region, which range from  $822$  to  $982 \text{ mm yr}^{-1}$  for Mato Grosso (Lathuillière et al., 2012; Priante-Filho et al., 2004). Measured evapotranspiration for soybean areas in Mato Grosso were unavailable, but Lathuillière et al. (2012) conducted an indirect measurement experiment with remote sensing products and crop modeling. Their estimates suggest that mean soybean evapotranspiration in Mato Grosso ( $540 \text{ mm yr}^{-1}$  or  $4.4 \text{ mm day}^{-1}$ , over the growing season) was lower than our simulated evapotranspiration for soybean ( $679 \text{ mm yr}^{-1}$ ). Our simulated soybean evapotranspiration may be higher than that of Lathuillière et al. (2012) because we included transpiration by soybeans during the growing season and evaporation throughout the year. Our simulated pasture and soybean evapotranspiration corresponded to 44% and 52%, respectively, of the mean precipitation.

Simulated evapotranspiration in agricultural ecosystems (pasture and soybean catchments) was about 39% lower than in natural ecosystems (forest and cerrado catchments). This is comparable to observed evapotranspiration reductions of about 36% following deforestation and pasture establishment in an area of Maranhão state (Oliveira et al., 2014).

Between April and August each year, the amount of precipitation was lower than the sum of evapotranspiration and total runoff (Fig. 5), indicating that vegetation was under water stress during this period. Unlike wet equatorial forests, where solar radiation availability is an important factor controlling evapotranspiration, seasonally dry tropical forests are largely controlled by seasonal trends in rainfall and the biotic response of plants to water stress (Costa et al., 2010; Vourlitis et al., 2008). The dry season was an equally important control on evapotranspiration in forest and cerrado ecosystems, consistent with previous studies (Biudes et al., 2015; Da Rocha et al., 2009; Rodrigues et al., 2014; Vourlitis et al., 2014). Evapotranspiration in perennial vegetation (forest, cerrado, and pasture) was somewhat greater during the dry season than the wet season, in response to the larger vapor pressure deficit, as previously reported by Costa et al. (2010). For soybeans, the growing season from November to February had greater evapotranspiration than the dry season.

Both observed and simulated results agree that the replacement of natural vegetation by agriculture increases streamflow by more than 100% in the Upper Xingu. Simulated mean annual total runoff for soybeans was twice that of forests ( $638$  and  $323 \text{ mm yr}^{-1}$ ).

Simulated subsurface runoff was 96% of annual total runoff in agricultural ecosystems and nearly 100% of annual total runoff in the natural ecosystems. These findings were consistent with the results reported by Hayhoe et al. (2011), who found that baseflow represented 96% of the discharge in forest and 94% of the discharge in soybean catchments in the Upper Xingu. However, the simulated subsurface runoff was highly seasonal, and reduced to near zero during the dry season (Fig. 5).

Agricultural ecosystems are generally expected to have larger surface runoff than natural ecosystems, which may cause environmental problems such as erosion and the loss of soil nutrients. However, the soil infiltrability and saturated hydraulic conductivity in this region were very high even after conversion of the landscape to agriculture. As a result, large soil infiltration and groundwater recharge – not increases in surface runoff – were the primary factor accounting for observed increases in total runoff in agricultural ecosystems. It is unclear whether other environmental problems may result from these increases in surface runoff. As noted by Neill et al. (2013), we do not yet know the full extent of areas with erosion nor the potential for increased erosion if a prolonged period of agriculture were to increase soil compaction in this region.

## 5. Conclusions

Observed and simulated results show that converting natural vegetation to agriculture substantially modifies the water balance components in small catchments in the Upper Xingu. Field observations indicated that mean streamflow in soy catchments was about three times greater than that of forest catchments, while the mean annual amplitude of observed flow was more than two times larger in soy than in forest areas.

Modeled results showed about 40% less evapotranspiration in agricultural ecosystems (pasture and soybean catchments) than in natural ecosystems (forest and cerrado catchments), whereas average

total discharge was about 100% higher in agricultural ecosystems than in natural ecosystems in the Upper Xingu.

Our study is a first step toward understanding the evapotranspiration and streamflow for four types of land cover in the study region. Future studies can investigate whether the consequences of increased water yield in headwater catchments can be detected in higher-order watersheds and how these cumulative disturbances might compromise the economic and environmental health of the Xingu River Basin. In situ data on soil parameters was essential to simulating the hydrologic behavior of this region. Therefore, future research should also focus on improving estimates of soil hydraulic properties in tropical soils, given the importance of these soil parameters for accurately simulating the water balance.

### Conflict of interest

No conflict of interest.

### Acknowledgments

We would like to acknowledge the Amazon Environmental Research Institute (IPAM) for weather station data and assistance with field data collection, as well as Grupo A. Maggi for providing access to the study site. We thank Shelby Riskin (nee Hayhoe), Richard McHorney, and Suzanne Spitzer for contributing and compiling streamflow data from Tanguro. This study was supported by the US National Science Foundation (DEB-0949996, DEB-0743703), the Gordon and Betty Moore Foundation, and the Conselho Nacional de Desenvolvimento Científico e Tecnológico (CNPq, process 135648/2011-4).

### References

- Aguiar, L.J.A., Costa, J.M.N., Fischer, G.R., Aguiar, R.G., Costa, A.C.L., Ferreira, W.P.M., 2011. Estimativa da radiação de onda longa atmosférica em áreas de floresta e de pastagem no sudoeste da Amazônia. *Rev. Bras. Meteorol.* 26, 215–224.
- Andréassian, V., 2004. Waters and forests: from historical controversy to scientific debate. *J. Hydrol.* 291, 1–27. <http://dx.doi.org/10.1016/j.jhydrol.2003.12.015>.
- Balch, J.K., Nepstad, D.C., Brando, P.M., Curran, L.M., Portela, O., de Carvalho, O., Lefebvre, P., 2008. Negative fire feedback in a transitional forest of southeastern Amazonia. *Glob. Chang. Biol.* 14, 2276–2287. <http://dx.doi.org/10.1111/j.1365-2486.2008.01655.x>.
- Ball, J.T., Woodrow, I.E., Berry, J.A., 1987. A model predicting stomatal conductance and its contribution to the control of photosynthesis under different light conditions. In: Biggins, J. (Ed.), *Progress in Photosynthetic Research*. Springer, Netherlands, Dordrecht, pp. 221–224.
- Barros, A.H.C., van Lier, Q.J., 2014. Pedotransfer functions for Brazilian soils. In: Teixeira, W.G., Ceddia, M.B., Ottoni, M.V., Donagema, G.K. (Eds.), *Application of Soil Physics in Environmental Analyses*. Springer International Publishing, pp. 131–162. [http://dx.doi.org/10.1007/978-3-319-06013-2\\_6](http://dx.doi.org/10.1007/978-3-319-06013-2_6).
- Biudes, M.S., Vourlitis, G.L., Machado, N.G., de Arruda, P.H.Z., Neves, G.A.R., de Almeida Lobo, F., Neale, C.M.U., de Souza Nogueira, J., 2015. Patterns of energy exchange for tropical ecosystems across a climate gradient in Mato Grosso, Brazil. *Agric. For. Meteorol.* 202, 112–124. <http://dx.doi.org/10.1016/j.agrformet.2014.12.008>.
- Bonan, G.B., Polard, D., Tompson, S.L., 1992. Effects of boreal forest vegetation on global climate. *Nature* 359, 716–718.
- Bosch, J.M., Hewlett, J.D., 1982. A review of catchment experiments to determine the effect of vegetation changes on water yield and evapotranspiration. *J. Hydrol.* 55, 3–23.
- Brown, A.E., Zhang, L., McMahon, T.A., Western, A.W., Vertessy, R.A., 2005. A review of paired catchment studies for determining changes in water yield resulting from alterations in vegetation. *J. Hydrol.* 310, 28–61. <http://dx.doi.org/10.1016/j.jhydrol.2004.12.010>.
- Bruijnzeel, L.A., 1990. *Hydrology of Moist Forest and the Effects of Conversion: A State of Knowledge Review*. UNESCO, Paris and Amsterdam.
- Brutsaert, W., 1975. On a derivable formula for long-wave radiation from clear skies. *Water Resour. Res.* 11, 742–744.
- Campbell, G.S., Norman, J.M., 1998. *An Introduction to Environmental Biophysics*, 2nd. ed. Springer, New York, NY. <http://dx.doi.org/10.1007/978-1-4612-1626-1>.
- Coe, M.T., Costa, M.H., Soares-Filho, B.S., 2009. The influence of historical and potential future deforestation on the stream flow of the Amazon River – Land surface processes and atmospheric feedbacks. *J. Hydrol.* 369, 165–174. <http://dx.doi.org/10.1016/j.jhydrol.2009.02.043>.
- Coe, M.T., Latrubesse, E.M., Ferreira, M.E., Amsler, M.L., 2011. The effects of deforestation and climate variability on the streamflow of the Araguaia River. *Brazil. Biogeochem.* 105, 119–131. <http://dx.doi.org/10.1007/s10533-011-9582-2>.
- Coe, M.T., Marthens, T.R., Costa, M.H., Galbraith, D.R., Greenglass, N.L., Imbuzeiro, H.M.A., Levine, N.M., Malhi, Y., Moorcroft, P.R., Muza, M.N., Powell, T.L., Saleska, S.R., Solorzano, L.A., Wang, J., 2013. Deforestation and climate feedbacks

- threaten the ecological integrity of south-southeastern Amazonia. *Philos. Trans. R. Soc. Lond. B. Biol. Sci.* 368, 20120155, <http://dx.doi.org/10.1098/rstb.2012.0155>.
- Cosby, B.J., Hornberger, G.M., Clapp, R.B., Ginn, T.R., 1984. A statistical exploration of the relationships of soil moisture characteristics to the physical properties of soils. *Water Resour. Res.* 20, 682–690, <http://dx.doi.org/10.1029/WR020i006p00682>.
- Costa, M.H., Biajoli, M.C., Sanches, L., Malhado, A.C.M., Hutyra, L.R., Da Rocha, H.R., Aguiar, R.G., De Araújo, A.C., 2010. Atmospheric versus vegetation controls of Amazonian tropical rain forest evapotranspiration: Are the wet and seasonally dry rain forests any different? *J. Geophys. Res. Biogeosci.* 115, 1–9, <http://dx.doi.org/10.1029/2009JG001179>.
- Costa, M.H., Foley, J.A., 1997. Water balance of the Amazon Basin: dependence on vegetation cover and canopy conductance. *J. Geophys. Res.* 102, 23973–23989.
- Costa, M.H., Foley, J.A., 2000. Combined effects of deforestation and doubled atmospheric CO<sub>2</sub> concentrations on the climate of Amazonia. *J. Clim.* 13, 18–34.
- Costa, M.H., Yanagi, S.N.M., Souza, P.J.O.P., Ribeiro, A., Rocha, E.J.P., 2007. Climate change in Amazonia caused by soybean cropland expansion, as compared to caused by pastureland expansion. *Geophys. Res. Lett.* 34, L07706, <http://dx.doi.org/10.1029/2007GL029271>.
- Cuenca, R.H., Ek, M., Mahrt, L., 1996. Impact of soil water property parameterization on atmospheric boundary layer simulation. *J. Geophys. Res.* 101, 7269–7277, <http://dx.doi.org/10.1029/95JD02413>.
- Da Rocha, H.R., Manzi, A.O., Cabral, O.M., Miller, S.D., Goulden, M.L., Saleska, S.R., R-Coupe, N., Wofsy, S.C., Borma, L.S., Artaxo, P., Vourlitis, G., Nogueira, J.S., Cardoso, F.L., Nobre, A.D., Kruijt, B., Freitas, H.C., von Randow, C., Aguiar, R.G., Maia, J.F., 2009. Patterns of water and heat flux across a biome gradient from tropical forest to savanna in Brazil. *J. Geophys. Res.* 114, G00B12, <http://dx.doi.org/10.1029/2007JG006640>.
- De Gonçalves, L.G.G., Borak, J.S., Costa, M.H., Saleska, S.R., Baker, I., Restrepo-Coupe, N., Muza, M.N., Poulter, B., Verbeeck, H., Fisher, J.B., Arain, M.A., Arkin, P., Cestaro, B.P., Christoffersen, B., Galbraith, D., Guan, X., van den Hurk, B.J.J.M., Ichii, K., Imbuzeiro, H.M.A., Jain, A.K., Levine, N., Lu, C., Miguez-Macho, G., Roberti, D.R., Sahoo, A., Sakaguchi, K., Schaefer, K., Shi, M., Shuttleworth, W.J., Tian, H., Yang, Z.-L., Zeng, X., 2013. Overview of the Large-Scale Biosphere–Atmosphere Experiment in Amazonia Data Model Intercomparison Project (LBA-DMIP). *Agric. For. Meteorol.* 182–183, 111–127, <http://dx.doi.org/10.1016/j.agrformet.2013.04.030>.
- Delire, C., Calvet, J., Noilhan, J., 1997. Physical properties of Amazonian soils: a modeling study using the Anglo-Brazilian Amazonian climate observation study data. *J. Geophys. Res.* 102, 119–130.
- Foley, J.A., Prentice, I.C., Ramankutty, N., Levis, S., Pollard, D., Sitch, S., Haxeltine, A., 1996. An integrated biosphere model of land surface processes, terrestrial carbon balance, and vegetation dynamics. *Global Biogeochem. Cycles* 10, 603–628.
- Giambelluca, T.W., Scholz, F.G., Bucci, S.J., Meinzer, F.C., Goldstein, G., Hoffmann, W.a., Franco, A.C., Buchert, M.P., 2009. Evapotranspiration and energy balance of Brazilian savannas with contrasting tree density. *Agric. For. Meteorol.* 149, 1365–1376, <http://dx.doi.org/10.1016/j.agrformet.2009.03.006>.
- Hayhoe, S.J., Neill, C., Porder, S., McHorney, R., Lefebvre, P., Coe, M.T., Elsenbeer, H., Krusche, A.V., 2011. Conversion to soy on the Amazonian agricultural frontier increases streamflow without affecting stormflow dynamics. *Glob. Chang. Biol.* 17, 1821–1833, <http://dx.doi.org/10.1111/j.1365-2486.2011.02392.x>.
- Hsu, K., Gao, X., Sorooshian, S., Gupta, H., 1997. Precipitation estimation from remotely sensed information using artificial neural networks. *J. Appl. Meteorol.* 36, 1176–1190.
- Idso, S.B., 1981. A set of equations for full spectrum and 8 to 14 μm and 10.5 to 12.5 μm thermal radiation from cloudless skies. *Water Resour. Res.* 17, 295–304.
- Idso, S.B., Jackson, R.D., 1969. Thermal radiation from the atmosphere. *J. Geophys. Res.* 74, 5397–5403.
- Kucharik, C.J., 2003. Evaluation of a Process-Based Agro-Ecosystem Model (Agro-IBIS) across the U.S. Corn Belt: Simulations of the Interannual Variability in Maize Yield. *Earth Interact.* 7, 1–33, [http://dx.doi.org/10.1175/1087-3562\(2003\)007<0001:EOAPAM>2.0.CO;2](http://dx.doi.org/10.1175/1087-3562(2003)007<0001:EOAPAM>2.0.CO;2).
- Kucharik, C.J., Foley, J.A., Delire, C., Fisher, V.A., Coe, M.T., Lenters, J.D., Young-Molling, C., Ramankutty, N., Norman, J.M., Gower, S.T., 2000. Testing the performance of a dynamic global ecosystem model: water balance, carbon balance, and vegetation structure. *Global Biogeochem. Cycles* 14, 795–825, <http://dx.doi.org/10.1029/1999GB001138>.
- Kucharik, C.J., Twine, T.E., 2007. Residue, respiration, and residuals: Evaluation of a dynamic agroecosystem model using eddy flux measurements and biometric data. *Agric. For. Meteorol.* 146, 134–158, <http://dx.doi.org/10.1016/j.agrformet.2007.05.011>.
- Lathuilière, M.J., Johnson, M.S., Donner, S.D., 2012. Water use by terrestrial ecosystems: temporal variability in rain-forest and agricultural contributions to evapotranspiration in Mato Grosso. Brazil. *Environ. Res. Lett.* 7, 1–12, <http://dx.doi.org/10.1088/1748-9326/7/2/024024>.
- Leite, C.C., Costa, M.H., de Lima, C.A., Ribeiro, C.A.A.S., Sedyama, G.C., 2011. Historical reconstruction of land use in the Brazilian Amazon (1940–1995). *J. Land Use Sci.* 6, 33–52, <http://dx.doi.org/10.1080/1747423X.2010.501157>.
- Lima, L.S., Coe, M.T., Soares Filho, B.S., Cuadra, S.V., Dias, L.C.P., Costa, M.H., Lima, L.S., Rodrigues, H.O., 2014. Feedbacks between deforestation, climate, and hydrology in the Southwestern Amazon: Implications for the provision of ecosystem services. *Landsc. Ecol.* 29, 261–274, <http://dx.doi.org/10.1007/s10980-013-9962-1>.
- Macedo, M.N., DeFries, R.S., Morton, D.C., Stickler, C.M., Galford, G.L., Shimabukuro, Y.E., 2012. Decoupling of deforestation and soy production in the southern Amazon during the late 2000s. *Proc. Natl. Acad. Sci. U. S. A.* 109, 1341–1346, <http://dx.doi.org/10.1073/pnas.1111374109>.
- Marthews, T.R., Quesada, C.A., Galbraith, D.R., Malhi, Y., Mullins, C.E., Hodnett, M.G., Dharssi, I., 2014. High-resolution hydraulic parameter maps for surface soils in tropical South America. *Geosci. Model Dev.* 7, 711–723, <http://dx.doi.org/10.5194/gmd-7-711-2014>.
- Morton, D.C., DeFries, R.S., Shimabukuro, Y.E., Anderson, L.O., Arai, E., del Bon Espirito-Santo, F., Freitas, R., Morissette, J., 2006. Cropland expansion changes deforestation dynamics in the southern Brazilian Amazon. *Proc. Natl. Acad. Sci. U. S. A.* 103, 14637–14641, <http://dx.doi.org/10.1073/pnas.0606377103>.
- Neill, C., Coe, M.T., Riskin, S.H., Krusche, A.V., Elsenbeer, H., Macedo, M.N., McHorney, R., Lefebvre, P., Davidson, E.A., Scheffler, R., Figueira, A.M.S., Porder, S., Deegan, L.A., 2013. Watershed responses to Amazon soy bean cropland expansion and intensification. *Philos. Trans. R. Soc. Lond. B. Biol. Sci.* 368, 20120425, <http://dx.doi.org/10.1098/rstb.2012.0425>.

- Oliveira, P.T.S., Nearing, M.A., Moran, M.S., Goodrich, D.C., Wendland, E., Gupta, H.V., 2014. Trends in water balance components across the Brazilian Cerrado. *Water Resour. Res.* <http://dx.doi.org/10.1002/2013WR015202>.
- Oliveira, R.S., Bezerra, L., Davidson, E.A., Pinto, F., Klink, C.A., Nepstad, D.C., Moreira, A., 2005. Deep root function in soil water dynamics in cerrado savannas of central Brazil. *Funct. Ecol.* 19, 574–581, <http://dx.doi.org/10.1111/j.1365-2435.2005.01003.x>.
- Panday, P.K., Coe, M.T., Macedo, M.N., Lefebvre, P., Castanho, A.D.D.A., 2015. Deforestation offsets water balance changes due to climate variability in the Xingu River in eastern Amazonia. *J. Hydrol.* 523, 822–829, <http://dx.doi.org/10.1016/j.jhydrol.2015.02.018>.
- Pollard, D., Thompson, S.L., 1995. Use of a land-surface-transfer scheme (LSX) in a global climate model: the response to doubling stomatal resistance. *Glob. Planet. Change* 10, 129–161, [http://dx.doi.org/10.1016/0921-8181\(94\)00023-7](http://dx.doi.org/10.1016/0921-8181(94)00023-7).
- Pongratz, J., Bounoua, L., DeFries, R.S., Morton, D.C., Anderson, L.O., Mauser, W., Klink, C.A., 2006. The impact of land cover change on surface energy and water balance in Mato Grosso. *Brazil. Earth Interact.* 10, 1–17, <http://dx.doi.org/10.1175/EI176.1>.
- Prata, A.J., 1996. A new long-wave formula for estimating downward clear-sky radiation at the surface. *Q. J. R. Meteorol. Soc.* 122, 1127–1151.
- Priante-Filho, N., Vourlitis, G.L., Hayashi, M.M.S., Nogueira, J.D.S., Campelo, J.H., Nunes, P.C., Souza, L.S.E., Couto, E.G., Hoeger, W., Raiter, F., Trienweiler, J.L., Miranda, E.J., Priante, P.C., Fritzen, C.L., Lacerda, M., Pereira, L.C., Biudes, M.S., Suli, G.S., Shiraiwa, S., Paulo, S.R.Do, Silveira, M., 2004. Comparison of the mass and energy exchange of a pasture and a mature transitional tropical forest of the southern Amazon Basin during a seasonal transition. *Glob. Chang. Biol.* 10, 863–876, <http://dx.doi.org/10.1111/j.1529-8817.2003.00775.x>.
- Rodrigues, T.R., Vourlitis, G.L., Lobo, F.D.A., De Oliveira, R.G., Nogueira, J.D.S., 2014. Seasonal variation in energy balance and canopy conductance for a tropical savanna ecosystem of south central Mato Grosso. *Brazil. J. Geophys. Res. Biogeosci.* 119, 1–13, <http://dx.doi.org/10.1002/2013JG002472>.
- Sahin, V., Hall, M.J., 1996. The effects of afforestation and deforestation on water yields. *J. Hydrol.* 178, 293–309, [http://dx.doi.org/10.1016/0022-1694\(95\)02825-0](http://dx.doi.org/10.1016/0022-1694(95)02825-0).
- Sampaio, G., Nobre, C., Costa, M.H., Satyamurty, P., Soares-Filho, B.S., Cardoso, M., 2007. Regional climate change over eastern Amazonia caused by pasture and soybean cropland expansion. *Geophys. Res. Lett.* 34, L17709, <http://dx.doi.org/10.1029/2007GL030612>.
- Satterlund, D.R., 1979. An improved equation for estimating long-wave radiation from the atmosphere. *Water Resour. Res.* 15, 1649–1650.
- Scheffler, R., Neill, C., Krusche, A.V., Elsenbeer, H., 2011. Soil hydraulic response to land-use change associated with the recent soybean expansion at the Amazon agricultural frontier. *Agric. Ecosyst. Environ.* 144, 281–289, <http://dx.doi.org/10.1016/j.agee.2011.08.016>.
- Sellers, P.J., Dickinson, R.E., Randall, D.A., Betts, A.K., Hall, F.G., Berry, J.A., Collatz, G.J., Denning, A.S., Mooney, H.A., Nobre, C.A., Sato, N., Field, C.B., Henderson-Sellers, A., 1997. Modeling the exchanges of energy, water, and carbon between continents and the atmosphere. *Science* 275, 502–509, <http://dx.doi.org/10.1126/science.275.5299.502>.
- Sellers, P.J., Los, S.O., Tucker, C.J., Justice, C.O., Dazlich, D.A., Collatz, G.J., Randall, D.A., 1996a. A revised land surface parameterization (SiB2) for atmospheric GCMs. Part II: The generation of global fields of terrestrial biophysical parameters from satellite data. *J. Clim.*, [http://dx.doi.org/10.1175/1520-0442\(1996\)009<0706:ARLSPF>2.0.CO;2](http://dx.doi.org/10.1175/1520-0442(1996)009<0706:ARLSPF>2.0.CO;2).
- Sellers, P.J., Randall, D.A., Collatz, G.J., Berry, J.A., Field, C.B., Dazlich, D.A., Zhang, C., Collelo, G.D., Bounoua, L., 1996b. A revised land surface parameterization (SiB2) for atmospheric GCMs. Part I: Model formulation. *J. Clim.*, [http://dx.doi.org/10.1175/1520-0442\(1996\)009<0676:ARLSPF>2.0.CO;2](http://dx.doi.org/10.1175/1520-0442(1996)009<0676:ARLSPF>2.0.CO;2).
- Sorooshian, S., Hsu, K., 2000. Evaluation of PERSIANN system satellite-based estimates of tropical rainfall. *Bull. Am. Meteorol. Soc.* 81, 2035–2046.
- Stickler, C.M., Coe, M.T., Costa, M.H., Nepstad, D.C., McGrath, D.G., Dias, L.C.P., Rodrigues, H.O., Soares-Filho, B.S., 2013. Dependence of hydropower energy generation on forests in the Amazon Basin at local and regional scales. *Proc. Natl. Acad. Sci. U. S. A.* 110, 9601–9606, <http://dx.doi.org/10.1073/pnas.1215331110>.
- Tomasella, J., Neill, C., Figueiredo, R., Nobre, A.D., 2009. Water and chemical budgets at the catchment scale including nutrient exports from intact forests and disturbed landscapes. In: Keller, M., Bustamante, M., Gash, J., Silva Dias, P. (Eds.), *Amazonia and Global Change*. American Geophysical Union, Washington, pp. 505–524.
- Vourlitis, G.L., de Souza Nogueira, J., de Almeida Lobo, F., Pinto, O.B., 2014. Variations in evapotranspiration and climate for an Amazonian semi-deciduous forest over seasonal, annual, and El Niño cycles. *Int. J. Biometeorol.*, <http://dx.doi.org/10.1007/s00484-014-0837-1>.
- Vourlitis, G.L., De Souza Nogueira, J., De Almeida Lobo, F., Sendall, K.M., De Paulo, S.R., Antunes Dias, C.A., Pinto, O.B., De Andrade, N.L.R., 2008. Energy balance and canopy conductance of a tropical semi-deciduous forest of the southern Amazon Basin. *Water Resour. Res.* 44, 1–14, <http://dx.doi.org/10.1029/2006WR005526>.
- Vourlitis, G.L., Priante-Filho, N., Hayashi, M.M.S., Nogueira, J.S., Caseiro, F.T., Campelo Jr., J.H., 2002. Seasonal variations in the evapotranspiration of a transitional tropical forest of Mato Grosso. *Brazil. Water Resour. Res.* 38, 1094.